J. Membrane Biol. 174, 59–70 (2000)

The Journal of
Membrane
Biology

Single-Channel Characterization of a Nonselective Cation Channel from Human Placental Microvillous Membranes. Large Conductance, Multiplicity of Conductance States, and Inhibition by Lanthanides

C. Grosman*, I.L. Reisin**

Departamento de Química Analítica y Fisicoquímica, Facultad de Farmacia y Bioquímica, Universidad de Buenos Aires, Buenos Aires (1113), Argentina

Received: 30 August 1999/Revised: 12 November 1999

Abstract. The rate-limiting step for the maternofetal exchange of low molecular-weight solutes in humans is constituted by transport across a single epithelial layer (syncytiotrophoblast) of the placenta. Other than the well-established presence of a large-conductance, multisubstate Cl^- channel, the ionic channels occurring in this syncytial tissue are, for the most part, unknown. We have found that fusion of apical plasma membrane-enriched vesicle fractions with planar lipid bilayers leads, mainly (96% of 353 reconstitutions), to the reconstitution of nonselective cation channels. Here we describe the properties of this novel placental conductance at the single-channel level. The channel has a large (>200 pS) and variable conductance, is cation selective ($P_{Cl}/P_K \cong 0.024$), is reversibly inhibited (presumably blocked) by submillimolar La^{3+}, has very unstable kinetics, and displays a large number (>10) of current sublevels with a "promiscuous" connectivity pattern. The occurrence of both "staircaselike" and "all-or-nothing" transitions between the minimum and maximum current levels was intriguing, particularly considering the large number of conductance levels spanned at a time during the concerted current steps. Single-channel data simulated according to a multistate linear reaction scheme, with rate constants that can vary spontaneously in time, reproduce many aspects of the recorded subconductance behavior. The channel's sensitivity to lanthanides is reminiscent of stretch-sensitive channels which, in turn, suggests a physiological role for this ion channel as a mechanotransducer during syncytiotrophoblast-volume regulation.

Key words: Syncytiotrophoblast — Epithelia — Channel reconstitution — Substates — Mechanosensitivity

Introduction

In the human placenta at term a single epithelial layer (syncytiotrophoblast) acts as the transport barrier for small molecules between the maternal and fetal bloodstreams. This tissue, unlike most other epithelia, forms a syncytium (Gaunt & Ockleford, 1986) i.e., a continuous, multinucleated cytoplasmic mass delimited by an apical (microvillous, maternal-facing) and a basal (fetal-facing) membrane without intercellular boundaries. The syncytium results from the fusion of individual cells (cytotrophoblast cells) during gestation. The syncytial nature of this epithelium suggests that the transport of ions and low-molecular weight hydrophilic solutes can only take place through the transcellular pathway, i.e., involving their translocation across both the apical and basal membranes. Nevertheless, the finding that the placental permeability to some hydrophilic molecules such as mannitol, sucrose, raffinose and inulin is approximately proportional to their diffusion coefficients in water, has been taken as an indication that paracellular pathways must also contribute to the maternofetal ion exchange (Stulč, 1989). Yet, there is still some debate about the existence of such alternative pathways because compelling structural evidences are lacking.

However, regardless of the extent to which the paracellular pathway contributes to the total transepithelial transfer of hydrophilic solutes, numerous transport pro-

* *Present address:* Department of Physiology and Biophysics, State University of New York at Buffalo, Buffalo, NY 14214, USA.

** Deceased

Correspondence to: C. Grosman

cesses are known to take place through the apical and basal membranes playing a role in transepithelial transport, and/or tissue homeostasis (Shennan & Boyd, 1987; Stulč, 1997; Sibley et al., 1998). The molecular mechanisms of these processes are little known. For instance, for many years the only available information about placental ion channels has been inferred from studies involving radiotracer-flux experiments (Byrne et al., 1993; Faller, O'Reilly & Ryan, 1994), membrane potential measurements (Greenwood, Boyd & Sibley, 1993), and partition of membrane potential-sensitive probes (Illsley & Sellers, 1992). It was only during the past few years that the first single-channel currents were recorded by applying the patch-clamp technique to both intact chorionic villi (Brown et al., 1993) and giant liposomes reconstituted with placental apical-membrane fragments (Riquelme et al., 1995). These single-channel studies led to the identification of a high-conductance, DIDS-sensitive Cl^- channel which, most likely, underlies the DIDS-sensitive component of the Cl^- conductance first revealed by radiotracer-flux studies (Byrne et al., 1993). More recently, we found (Grosman & Reisin, 1996) that the planar lipid bilayer reconstitution technique is also a valuable tool for studying the ionic channels present in the microvillous membrane of the syncytiotrophoblast which, because of its highly irregular surface, offers a difficult access to the conventional patch-clamp technique (Brown et al., 1993). We reported (Grosman et al., 1997) that the reconstitution technique led to the incorporation of an overwhelming majority (96% of 353 reconstitutions) of nonselective cation channels in addition to the maxi-Cl^- channel previously revealed by patch-clamp studies (Brown et al., 1993; Riquelme et al., 1995), and to an apparently novel Cl^- channel (~100 pS in symmetrical 295 mM Cl^-). Previous patch-clamp studies have made little (Riquelme et al., 1995, 1999) or no (Brown et al., 1993) comments on placental cationic conductances. This paper characterizes some conductive and gating properties of this novel placental nonselective cation channel emphasizing its complex kinetics, the multiplicity of conductance states, and the inhibition by submillimolar La^{3+}. In particular, the sensitivity to lanthanides is reminiscent of mechanosensitive channels which, in turn, suggests a role in cell-volume regulation for this ion channel.

Materials and Methods

Microvillous Membrane Vesicle Preparation and Characterization

The method outlined by Booth, Olaniyan and Vanderpuye (1980) was followed with some minor modifications, as previously described (Grosman et al., 1997). Briefly, full term, normal human placentas were obtained within 20 min of vaginal delivery (University of Buenos Aires Hospital), in agreement with institutional guidelines, and were immediately processed. All steps were carried out at 0–4°C. Villous tissue was fragmented, washed with unbuffered 150 mM NaCl, and cut into small pieces. A given amount of tissue was agitated with a magnetic stirrer for 1 hr in 1.5 volumes of a 10-mM HEPES-KOH, pH 7.4 buffer solution containing 0.1 mM EGTA, 0.2 mM phenylmethylsulfonyl fluoride, and either 150 mM NaCl, 250 mM sucrose or 150 mM KI as homogenization buffer osmolytes. The agitated tissue was poured through several layers of cheesecloth, and the filtrate was used to prepare a microsomal fraction by differential centrifugation. Apical plasma membrane fragments were separated from nonapical membranes (i.e., basal plasma membrane, and intracellular membrane fragments present in the microsomes) by selectively precipitating the latter with 10 mM $MgCl_2$. The final membrane suspension was then aliquoted, stored at −20°C, and assayed for biochemical and morphological markers. Both marker enzyme analysis and electron microscopy indicated that the isolated membrane fraction is enriched in apical plasma membranes with no significant subcellular contaminants (Grosman et al., 1997). The alkaline phosphatase activity (an apical plasma membrane enzymatic marker) in the final membrane suspension normalized to that in the filtrate was >20 while these ratios for enzymes that are markers of nonapical membranes were <1.5. Marker enzyme analysis, polyacrylamide gel electrophoresis in sodium dodecyl sulfate, electron microscopy, and ion channel reconstitution suggested that the fractions obtained using either homogenization buffer osmolyte were indistinguishable (Grosman et al., 1997).

Channel Reconstitution

Lipid bilayers were formed by using different mixtures of synthetic phospholipids (Avanti Polar Lipids, Birmingham, AL) with or without cholesterol (recrystallized in ethanol) in *n*-decane. All the phospholipids used were 1-palmitoyl-2-oleoyl-based, the polar head group being either choline (POPC), ethanolamine (POPE) or serine (POPS). The lipid solution (~20–25 mg/mL) was spread over a 250-μm diameter aperture in a polystyrene cuvette by means of a thin glass or plastic rod. The cuvette was inserted into one of a pair of pits machined on a polyvinyl chloride holder thus defining two aqueous compartments (800 and 1600 μL) separated by a planar lipid film, as described by Alvarez, Benos and Latorre (1985). At the beginning of every experiment both sides of the bilayer were bathed by a solution containing 10–15 μM Ca^{2+} and 10 mM MOPS-KOH, pH 7.4 ($[K^+] \cong 5$ mM). The solution in the *cis* side (the one into which the membrane vesicles were added) also contained 145 mM KCl. Thus, the *cis* compartment was 150 mM in K^+ and 145 mM in Cl^- whereas the *trans* side was just ~5 mM in K^+. Once a successful channel insertion took place, appropriate volumes of concentrated solutions were added to either side of the bilayer to achieve the desired solute concentration, as stated in the text. Otherwise stated, all chemicals were purchased from Sigma Chemical, St. Louis, MO.

Electrical Recordings

Voltage was applied to the *trans* solution with either a DC voltage source or a function generator. The opposite side, *cis*, was defined as virtual ground. Nevertheless, throughout the paper, the *cis* minus *trans* voltage is indicated. Electrical contacts were made through Ag/AgCl electrodes and 200-mM KCl, 2% (w/v) agar bridges. The current across the bilayer was recorded using a current-to-voltage converter with a 10-GΩ-feedback resistor. The output voltage was low-pass filtered at 1 kHz (−3dB) with an eight-pole, Bessel-type filter (Frequency Devices, Haverhill, MA), digitized with a pulse code modulator, stored on video tapes with a VCR, and acquired (offline) at 4 kHz for subsequent

analysis. Current traces shown in Results were further filtered (Gaussian digital filter), for display purposes, and the overall cutoff frequency (cascaded filters) was 450 Hz (−3 dB). Bilayer formation was monitored by applying a 2.5-mV-peak-to-peak, 20-Hz, triangular wave. Typically, 100–200-pF bilayers were obtained. All the experiments were performed at room temperature (20–25°C).

Single-Channel Data Acquisition, Analysis and Simulation

pClamp Version 5.5 (Axon Instruments, Foster City, CA), and SigmaPlot Version 4.02 (Jandel Scientific, Corte Madera, CA) programs were used for acquisition and analysis of experimentally derived data. A single-channel simulation program of our own design was used to generate the data in Fig. 8.

Results

Analysis of Single-Channel Recordings

A vesicle fraction enriched (more than twentyfold) in apical plasma membranes from the human syncytiotrophoblast was assayed for the presence of ion channels by reconstitution on planar lipid bilayers. Most (96% of 353) of the reconstitutions led to the insertion of channels whose electrical behavior is shown in Fig. 1. Each panel of current traces (*A–D*) corresponds to a different experiment, and illustrates the channel's activity at different voltages and under the same ionic conditions (150 mM K^+, 145 mM Cl^- in *cis*, and 5 mM K^+ in *trans*). The abundance of ill-defined current sublevels and the highly variable behavior recorded both during a given experiment and from bilayer to bilayer (Figs. 1, 2, 3 and 4) made difficult the quantitative characterization and the unequivocal identification of this channel once a successful reconstitution took place. Thus, we considered that collecting data from a large number of experiments was a reasonable way of dealing with this problem. The data presented in this paper is representative of the results obtained in 339 single-channel reconstitutions.

Four functional characteristics were used as "fingerprints" for channel identification: (i) cationic selectivity, (ii) large conductance, (iii) highly variable kinetics, and (iv) complex subconductance organization. In most of the experiments the currents were very irregularly shaped to the extent that, for certain periods of time, they seemed to arise from the independent activity of several coreconstituted low-conductance ion channels. This situation is exemplified in some of the traces in Figs. 1*A* and *B.* However, even a qualitative visual analysis of *all* the traces in Figs. 1, 2, and 3 is enough to rule out this possibility. For example, current steps spanning several conductances levels at a time (data displayed at 450 Hz bandwith and 4 kHz sampling rate) were frequently observed. The probability of this finding occurring just as a result of a coincidence decreases monotonically as the number of conductance levels involved in a current step increases, a situation that contrasts with the observed single-channel data. Also, the frequent observation of long-lived (up to seconds) silent sojourns in the minimum, maximum, or some of the intermediate conductance levels argues against the multichannel nature of the bilayers. In summary, these observations allow us to assert that all the information presented in this paper corresponds to single channels.

Figure 4 illustrates another unusual characteristic of this channel: the bilayer to bilayer variability of the maximum conductance reached. The current steps shown were recorded in three different experiments with 150 mM K^+ and 145 mM Cl^- in the *cis* side, and 5 mM K^+ in the *trans* side. These current steps indicate the maximum current attained at the indicated voltage in each experiment.

The reversal potential when the bilayer was bathed by 150 mM K^+ and 145 mM Cl^- in the *cis* side, and 5 mM K^+ in the *trans* side was close to −80 mV, the K^+ Nernst potential under such ionic conditions. Occasionally, the reversal potential appeared shifted towards less negative potentials but the addition of 1-mM DIDS "corrected" this shift. This finding was interpreted as the blockade of coreconstituted, low-conductance Cl^- channels that, in the absence of the blocker, allowed Cl^- ions from the *cis* compartment to carry some (negative) current at negative potentials (*trans* is taken as ground). Figure 5 shows the current-voltage (*I-V*) relationships under asymmetric ionic conditions obtained from the analysis of ten independent bilayers. Due to the difficulties encountered to define a main conductance level in a given bilayer, to the conductance variability from experiment to experiment, and to the occurrence of what sometimes appeared to be a continuous spectrum of current sublevels, the *I-V* data points were obtained according to the following (arbitrary) procedure. Every single-channel trace was segmented in 19-sec long intervals. The maximum current-amplitude value attained in each of these intervals was assigned a data point in the *I-V* plot. Additionally, every 19-sec long interval was further divided in 512-msec long periods. Any current value that for four consecutive 512-msec periods was the largest (even when being lower than the maximum value of the corresponding 19-sec interval) was also included as a data point in the curve. Thus, these *I-V* relationships include information about the largest-conductance states. We used the program FETCHAN (pClamp software) for the estimation of the different current levels. Current recordings (fc = 450 Hz, 512 msec/sweep) were browsed and horizontal cursors were manually placed at positions that fitted best (by eye) the clearest current levels. Fitting all-point current-amplitude histograms to mixtures of Gaussian densities usually provides a much more objective means to interpret the subconductance organization of a multisub-

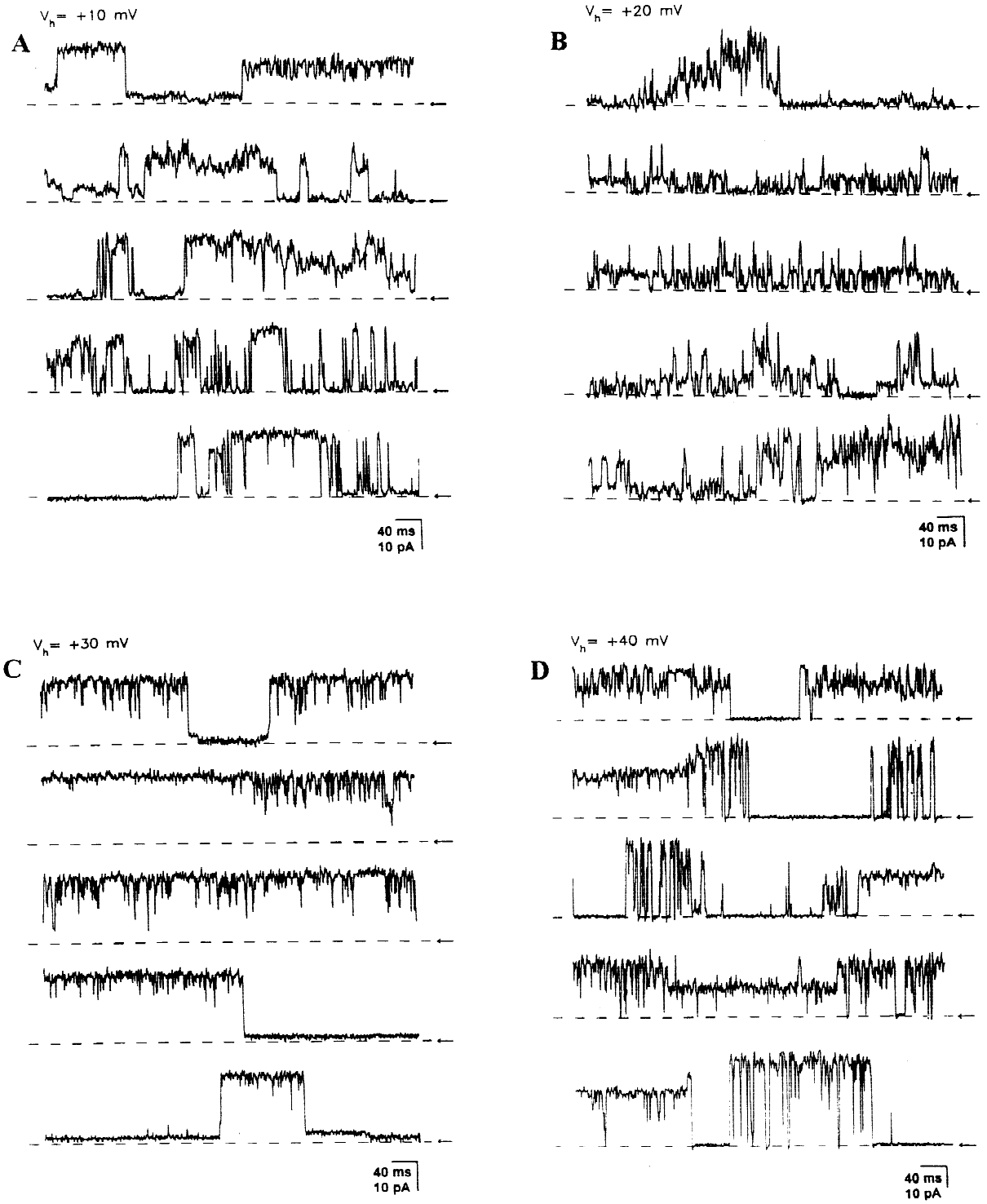

Fig. 1. Selected single-channel current traces from the placental nonselective cation channel. (*A–D*) Panels of continuous current traces corresponding to four independent bilayers at different voltages. Arrowheads indicate the closed state. Note the different current-amplitude scale for panel *D*.

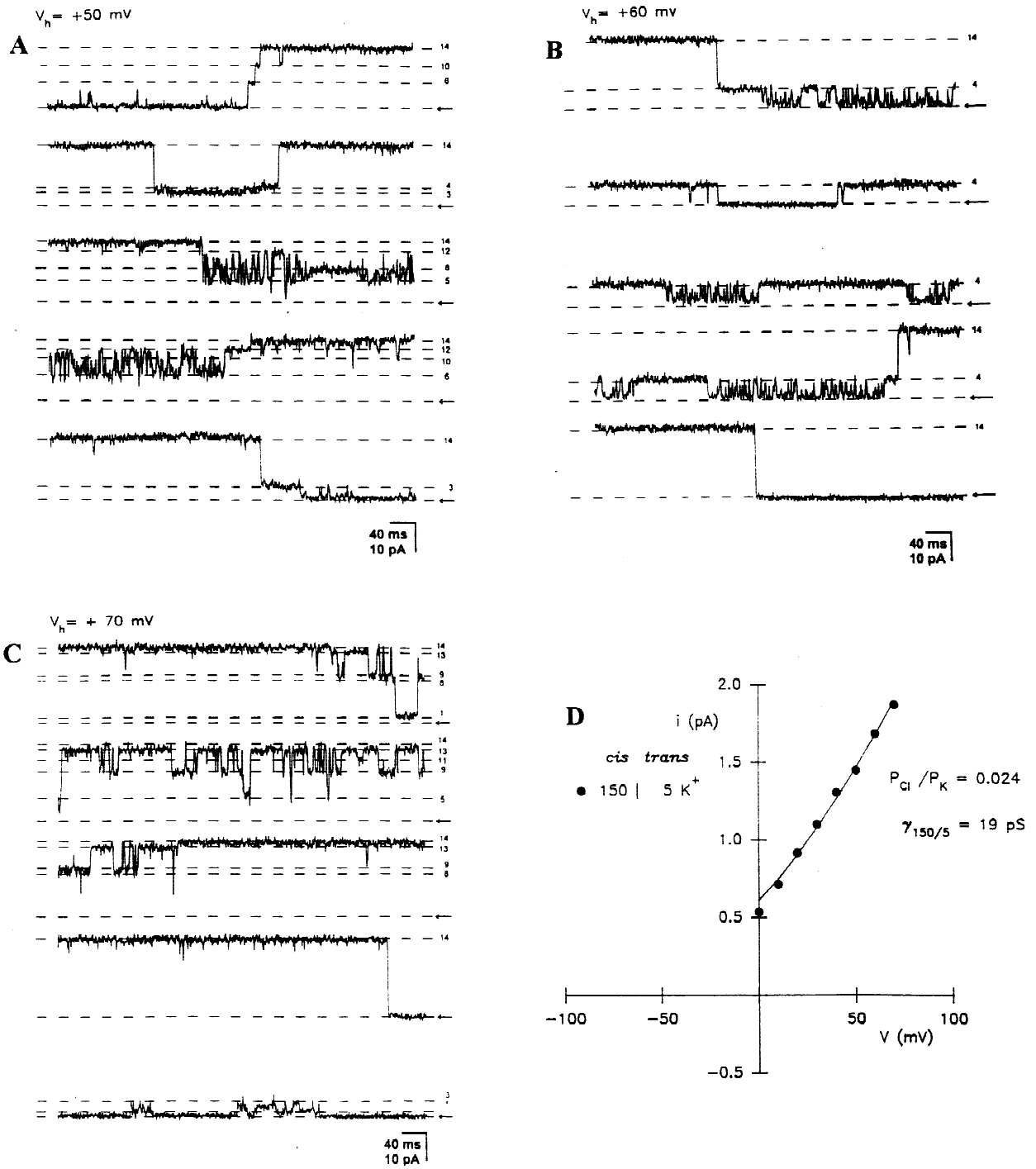

Fig. 2. Multiplicity of conductance states. (*A–C*) Panels of continuous current traces recorded from the same bilayer at different voltages. Note the abundance and complexity of sojourns in subconductance states. Arrowheads indicate the closed state. (*D*) *I-V* profile of a putative 19-pS elementary unit.

state channel (Krouse, Schneider & Gage, 1986; Hunter & Giebisch, 1987). However in the present case, as it was in the placental maxi-Cl^- channel's (Grosman et al., 1997), the unfavorable signal to noise ratio of the current sublevels blurred the current-amplitude histograms to the extent that they appeared as single, broad peaks that could not be fitted to Gaussian densities.

In an attempt to regulate the activity of this ion

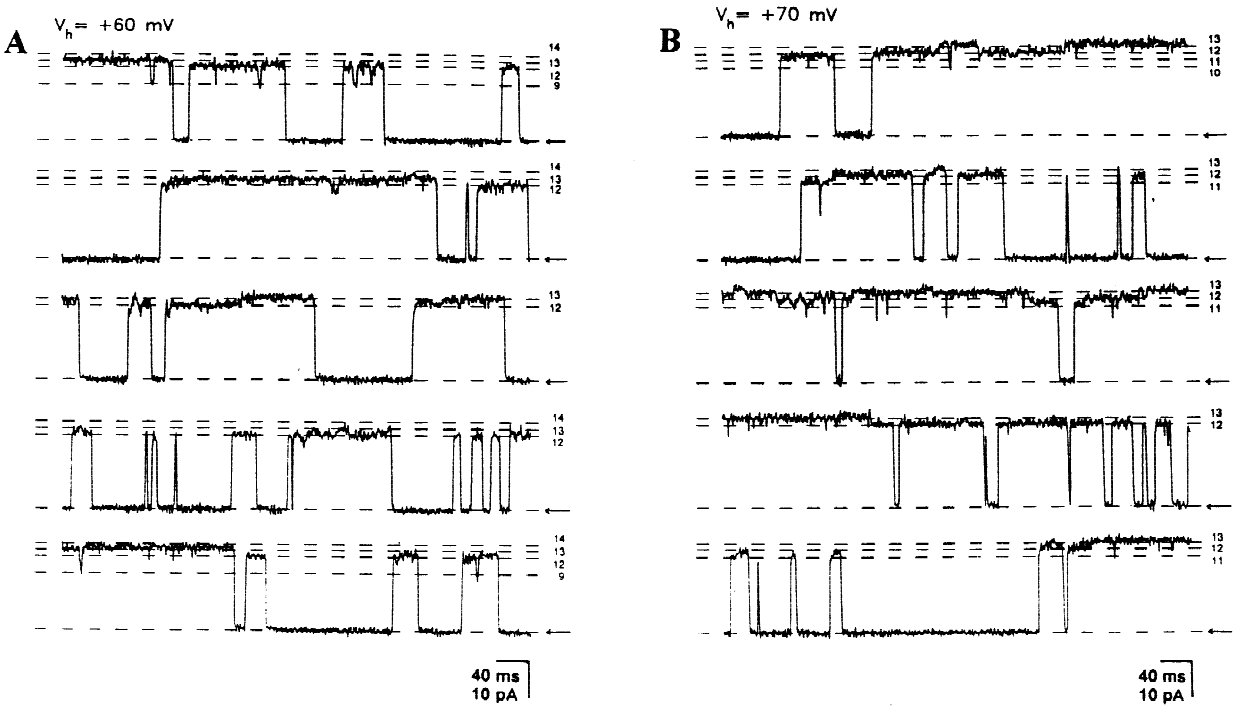

Fig. 3. Different gating modes. Single-channel currents in *A* and *B* were recorded from the same bilayer as, and some seconds after, those shown in Fig. 2. Note the spontaneous switch from a gating behavior characterized by frequent sojourns in subconductance states (Fig. 2) to one during which concerted current steps predominated. Arrowheads indicate the closed state.

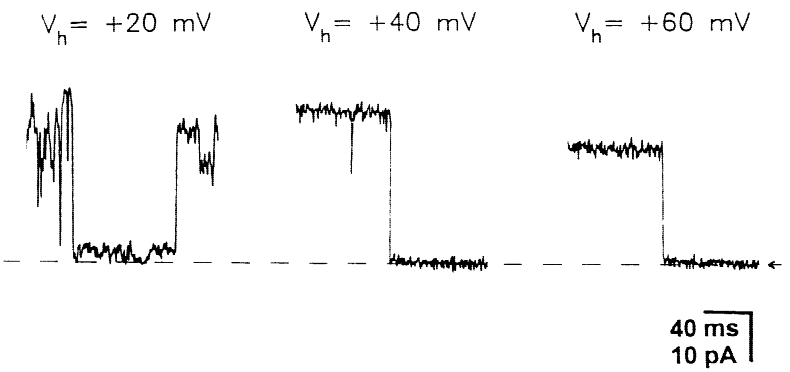

Fig. 4. Single-channel conductance variability between bilayers. Example current steps recorded in three different bilayers showing the highest conductance attained in each case. Currents are shown at different voltages to emphasize the variable conductance. The arrowhead indicates the closed state.

channel, a variety of inorganic ions and organic compounds were added to the solutions bathing the bilayer. The addition of Mg^{2+}, Ca^{2+}, or Ba^{2+} to the *cis* side up to 1 mM did not affect the general behavior of the channel. The reduction of Ca^{2+} concentration in either chamber (initially 10–15 μM) down to subnanomolar concentrations (upon addition of 1 mM EDTA) also failed to alter the activity of the reconstituted channels. In contrast, micromolar concentrations of $LaCl_3$ reversibly reduced the activity of the channel (Fig. 6) being effective only from one side of the bilayer. The La^{3+}-sensitive side of the channel was not always exposed to the same aqueous compartment (*cis* or *trans*), a fact that most likely was due to the existence of vesicles with different orientation (right side-out or inside-out). As shown in Fig. 6, in the presence of 100 μM La^{3+} the current dropped to virtually zero. The figure also shows that addition of 1 mM EDTA (its affinity constant for La^{3+} at pH 7.4 is ~3.3×10^{12} M^{-1}) reverted this effect. Among organic compounds, tetraethylammonium chloride (10 mM), heptanol (7 mM), or ryanodine (20 μM) added to either or both sides of the bilayer did not exert any obvious effect on the channel's activity. As shown in Figs. 1, 2, and 3, the potential difference across the membrane also failed to regulate the behavior of this channel.

To learn about the role played by the surface charge and stiffness of the lipid bilayer on the behavior of the channel, we tested bilayers of varying compositions.

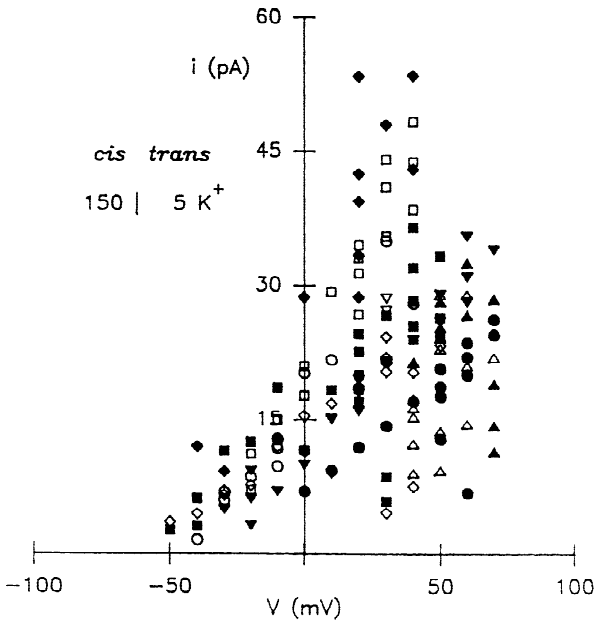

Fig. 5. *I-V* profile. Current amplitudes were estimated according to a procedure indicated in the text. The procedure was aimed at including information about the largest-conductance current levels i.e., those that were most reliably measured. Every symbol type identifies a set of values obtained from the same bilayer. The plot includes data from ten independent bilayers.

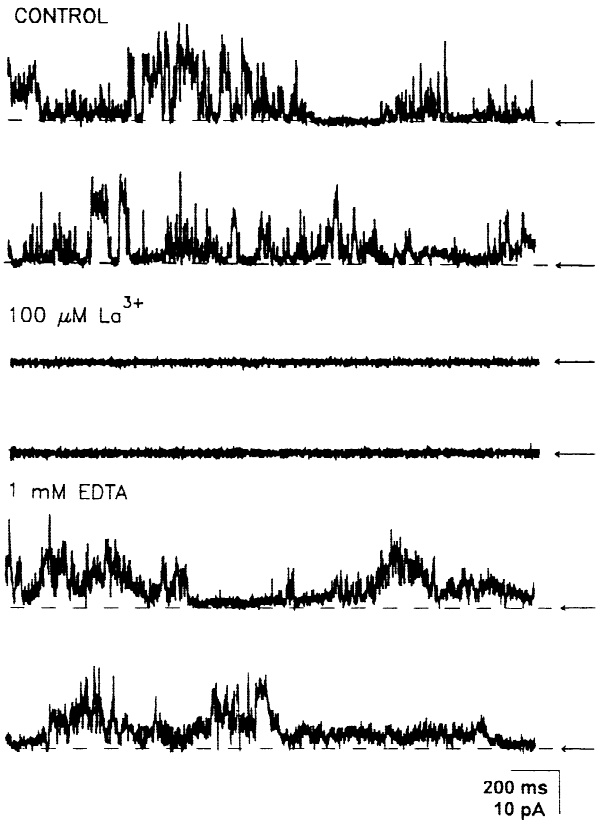

Fig. 6. Inhibition by La^{3+}. Channel currents (V_h = +40 mV) sequentially recorded under control conditions (top two traces), in the presence of 100 μM La^{3+} (middle two traces), and with 1 mM EDTA added (bottom two traces). Arrowheads indicate the closed state.

The lipids used were: POPE (neutral), POPC (neutral), POPS (negatively charged), and cholesterol (to increase the bilayer's stiffness). The different combinations tested were: POPE:POPC, 7:3 (the combination used in all the traces shown in this paper); POPE:POPC:cholesterol, 5:2.1:2.9, and 6.2:2.6:1.2; and POPE:POPS:cholesterol, 6.2:2.6:1.2, all dissolved in *n*-decane. The activity of the channel appeared to be oblivious to the particular composition of the bilayer.

Figures 2 and 3 show current traces recorded at different voltages from the same single-channel-containing bilayer. Figure 3 traces were recorded some seconds after those in Fig. 2. These figures clearly show two spontaneously occurring gating modes: while subconductance sojourns are frequent in Fig. 2, single-channel currents in Fig. 3 occur, for the most part, as "all-or-nothing," concerted steps. These recordings best illustrate the general functional characteristics of the placental cation channel: discrete subconductances, heterogeneous kinetics of main and substates, and both concerted and "staircase-like" (sequential) openings and closures. In this particular bilayer, sojourns in the various current levels were longer-lived than those shown in Fig. 1, which made their visual analysis more reliable. The close inspection of these traces (the same analysis as for Fig. 1) allowed us to identify fourteen nearly equally spaced current sublevels. The *I-V* relationship of the elementary conductance under asymmetric ionic conditions is shown in Fig. 2*D*. A fit of the experimental points to a straight line has a slope of 19 pS. The extrapolated reversal potential, calculated from a fit of the experimental points to a second-order polynomial (solid line), indicated that $P_{Cl}/P_K \cong 0.024$. This fit was preferred over a fit to a straight line because it captured, at least in part, the rectification clearly observed under the asymmetric ionic conditions used. It was difficult, however, to reliably quantify current amplitudes that were smaller than 0.5 pA and, therefore, they do not appear in the *I-V* plot. By no means are these results meant to characterize all the single-channel currents recorded in the 339 successful reconstitutions but, at least, a model of fourteen 19-pS elementary conductances (260–270 pS total) fitted well the data in Figs. 2 and 3. A similar analysis was attempted in several other sets of traces (as those in Fig. 1, for example) but the reliability of the results was always questionable. Figure 2 also shows that the dwell-times in the different current levels are highly heterogeneous, suggesting that their distributions are best described by mixtures of several exponential densities rather than by single components.

As mentioned above, current transitions (both openings and closures) between any two conductance-levels

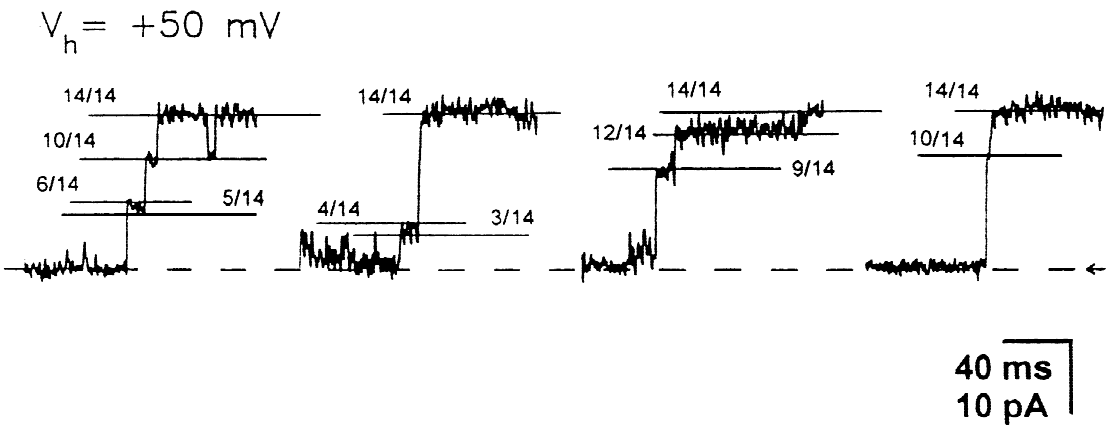

Fig. 7. Sequential *vs.* concerted openings recorded in the same bilayer. The horizontal lines identify the different conductance levels expressed as fractions of their total number. The arrowhead indicates the closed state.

occurred either as single, all-or-nothing steps or as a series of smaller current steps in quick succession ("sequential"). Figure 7 shows an example of this behavior for four channel openings going from the totally closed to the maximum open level reached during this particular recording. All four openings correspond to the same bilayer steadily clamped at +50 mV, under the same ionic conditions. The figure emphasizes that the size (and, therefore, the number) of sequential steps needed to reach the fully open level was highly variable, even within the same experiment. This same sequential/concerted pattern was also observed during channel closures.

A Reaction Scheme

A close inspection of the recorded single-channel traces suggested that most (if not all) of the different conductance levels are "connected" to each other. This apparently simple finding represents an interesting problem as far as the underlying reaction scheme is concerned, particularly when the number of subconductances present is large. The most straightforward model that can account for such "promiscuous" state connectivity is one that has (at least) as many states as different conductances, it is fully connected, and it is time homogeneous (i.e., the rate constants do not vary with time). According to this mechanistic view, every current step between any two conductance levels reflects a distinct conformational change that is independent of those linking all the other pairs of states. Thus, all-or-nothing current transitions between the fully closed and fully open current levels would result from a single conformational change while sequential current transitions between those two states (exemplified in Fig. 7) would reflect a series of unrelated conformational changes that happen to occur in quick succession. For a channel with few sublevels this model may be satisfactory, but it is the large number of connections required in the case of the placental channel what makes this model little likely from a physical viewpoint. For example, for a channel having ten conductances (including the zero-current level), this model requires as many as forty-five independent conformational changes (i.e., ninety rate constants). Of course, it is not the large number of rate constants itself what makes this model improbable but the structural complexity predicted by it. An alternative model, which is more parsimonious and seems to be more physically plausible, was then considered. According to this hypothetical mechanism, the channel has two major conformational states that correspond to the totally open and totally closed channel. In its transition between these two states, the channel "visits" a series of intermediate conformations which account for the subconductances. When the sojourns in these intermediate states are very brief, the full opening (or full closing) of the channel is manifest as an all-or-nothing switch. In contrast, when the channel lingers on intermediate conformations, the transition appears as a stepwise change with detectable sublevels. This model also consists of (at least) as many states as different conductances but these are arranged in a linear scheme which, for the ten-conductance model of our example, implies nine conformational changes and, therefore, only eighteen rate constants. The ability of this linear model to predict the recorded data was tested by simulating single-channel currents. The following kinetic scheme was used:

$$\overset{\text{I}}{C} \rightleftharpoons \overset{\text{II}}{S_1} \rightleftharpoons \overset{\text{III}}{S_2} \rightleftharpoons \overset{\text{IV}}{S_3} \rightleftharpoons \overset{\text{V}}{S_4} \rightleftharpoons \overset{\text{VI}}{S_5} \rightleftharpoons \overset{\text{VII}}{S_6} \rightleftharpoons \overset{\text{VIII}}{S_7} \rightleftharpoons \overset{\text{IX}}{S_8} \rightleftharpoons O$$

where C and O denote the fully closed and fully open states of the channel, respectively, S_1 to S_8 represent the eight substates, and the roman numerals identify the nine isomerization steps. Only for interpretation convenience we will assume, in what follows, that this hypothetical channel is formed by nine identical monomers (either

Table 1. Single-channel transition rates used for simulation

Scheme	Rate*	Isomerization step								
		I	II	III	IV	V	VI	VII	VIII	IX
A	Forward	100	80,000	70,000	60,000	50,000	40,000	30,000	20,000	10,000
	Backward	10,000	20,000	30,000	40,000	50,000	60,000	70,000	80,000	100
B	Forward	100	50,000	50,000	50,000	50,000	50,000	50,000	50,000	50,000
	Backward	50,000	50,000	50,000	50,000	50,000	50,000	50,000	50,000	100
C	Forward	100	2,500	2,500	2,500	2,500	2,500	2,500	2,500	2,500
	Backward	2,500	2,500	2,500	2,500	2,500	2,500	2,500	2,500	100
D	Forward	100	1,000	1,000	1,000	1,000	1,000	1,000	1,000	1,000
	Backward	1,000	1,000	1,000	1,000	1,000	1,000	1,000	1,000	100
E	Forward	500	500	500	500	500	500	500	500	500
	Backward	500	500	500	500	500	500	500	500	500
F	Forward	100	50,000	50,000	50,000	50,000	50,000	250	50,000	50,000
	Backward	250	50,000	50,000	50,000	50,000	50,000	50,000	50,000	100

* All rates are given in sec^{-1}

subunits lining a single pore or protochannels each lining an individual pore of a multibarreled channel) each of which can undergo a binary closed $\rightleftharpoons$ open conformational change. Thus, *C* and *O* correspond to the two homomeric configurations (all monomers closed or all of them open, respectively) whereas each *Sn* represents the set of equivalent heteromeric structures with *n* monomers in the open conformation. Based on the results obtained during the reconstitution experiments, we assumed that the opening of every additional monomer contributes with the same elementary conductance. Different sets of rate constants were simulated to test the validity of the model and to get an order-of-magnitude idea of the values of the rate constants between states. The kinetic parameters and results of six such simulations are shown in Table 1 and Fig. 8, respectively. The rate constants in Table 1 are "macroscopic" or "statistically corrected" in the sense that they reflect the number of hypothetical monomers that can undergo a given isomerization step. In schemes *A, B, C, D,* and *F* both the fully closed and fully open states are particularly stable, a characteristic that is needed to account for the long sojourns usually observed in these states. These five schemes differ, however, in the remaining rate constants. In scheme *A,* once the channel reaches S_1 or S_8 the eight remaining subunits behave independently of each other, opening and closing at a (microscopic) rate of 10,000 sec^{-1} per subunit. This scheme predicts some "flickery" gating around 50% of the total amplitude. This is hardly surprising because only for S_4 and S_5 the two transition rates leading away from them are very similar to each other (40,000 and 50,000 sec^{-1}). Thus, once any of these sublevels is reached, the probabilities of further opening or closing are almost equivalent ($P \cong 0.5$). In contrast once S_2 is reached, for example, the channel proceeds to S_3 with a probability of ~0.78 (and to S_1 with $P \cong 0.22$) which makes S_3 a more populated substate than S_1. For the same reason S_6 is more populated than S_8. By generalizing this concept we conclude that, except from the long sojourns in *C* and *O*, the channel spends longer in S_4 and S_5 not because they are longer lived (all the subconductances have the same mean lifetime of ~11 μsec) but because they are visited more often. The fact that such behavior was practically absent from the recordings (flickery transitions were recorded but not necessarily around 50% of the total amplitude) indicates that scheme A is inappropriate. In schemes *B, C, D,* and *E* the statistically corrected transition rates for opening or closing are the same from all the substates as if the opening (or closing) of one subunit increased the microscopic rate of opening (or closing) of the remaining subunits. This incorporation of positive cooperativity greatly improved the ability of the linear model to mimic the experimentally derived data. Scheme B predicts the occurrence of concerted openings and closures like those shown in Figs. 2, 3, and 4. It is also remarkable how well it predicts the existence of brief spikes of currents. Because of the fast transition rates between subconductance levels (50,000 sec^{-1}), every sequence of current transitions that starting at the closed level does not reach the fully open level and, instead, goes back to closed (or *vice versa*), gives rise to one such spikes many of which go undetected. The fine kinetic structure of these brief current transitions is better illustrated in Fig. 8*C–E,* where the rates between sublevels are considerably smaller. Schemes *C–E* succeed in predicting the existence of longer-lived sojourns in intermediate conductance levels, and the frequent occurrence of sequential openings and closures of the type shown, most notably, in Fig. 7. Finally, scheme *F* predicts the type of flickery behavior better illustrated in Fig. 2*B.* This scheme is basically scheme *B* but the $S_1 \rightarrow C$ and $S_6 \rightarrow S_7$ transitions are made much slower so that the currents adopt the form of bursts of activity between S_1 and S_6 interrupted by longer-duration dwellings in *C* and *O.* These bursts are far from being simple,

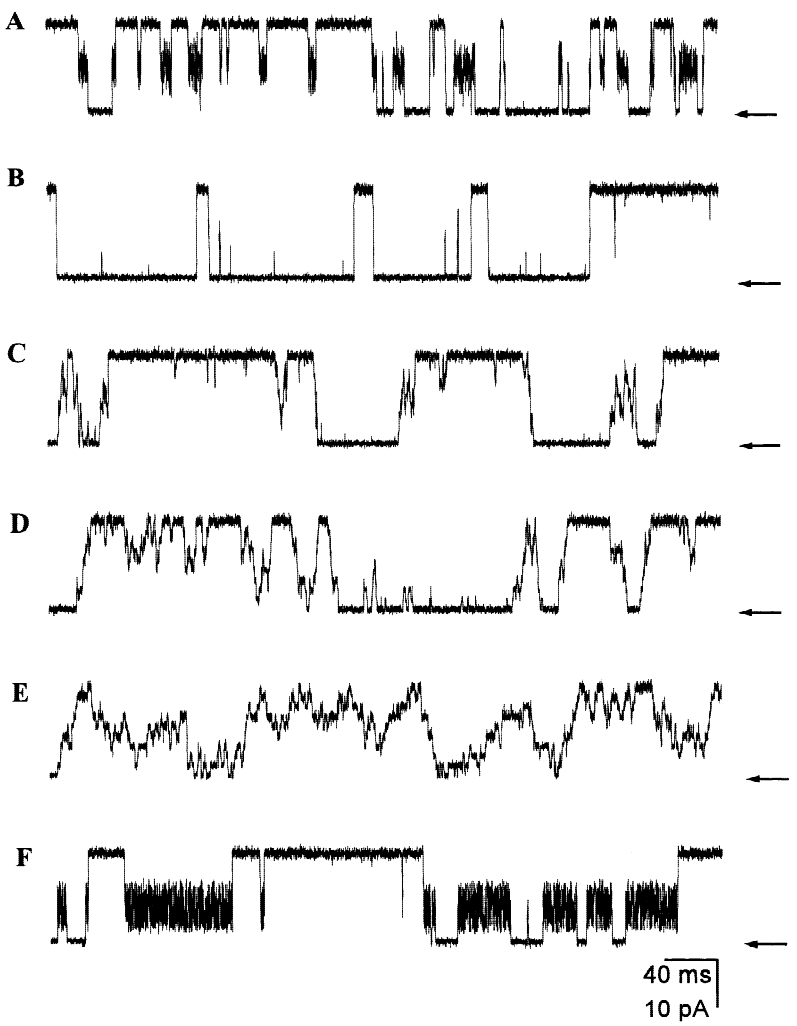

Fig. 8. Simulated single-channel data according to a linear multistate reaction scheme. The transition rates are indicated in Table 1. The current-step size and root mean square (rms) excess noise between any two adjacent conductance levels were 2 pA and 0.46 pA, respectively. The rms noise of the zero-current level (baseline) was 1 pA. Currents were simulated, and are displayed at, a sampling rate of 100 kHz and a filter cutoff (Gaussian digital filter) of 50 kHz.

two-state transitions between S_1 and S_6. From the transition rates in Table 1, it can be calculated that each such burst has a rather complex kinetics consisting, on average, of 100.5 sojourns in S_1 and S_6, 200 in S_2, S_3, S_4, and S_5, and 1 in S_7 and S_8, and has a mean duration of 12 msec.

In conclusion, a multistate linear kinetic scheme with transition rates that can spontaneously vary seems to capture several aspects of the gating kinetics of this novel cation-selective channel.

Discussion

Channel Reconstitution

To the best of our knowledge, this paper provides the first electrophysiological evidence for the existence of a nonselective cation conductance in the microvillous membrane of the human syncytiotrophoblast at term. The fusion of plasma membrane vesicles to planar lipid bilayers turned out to be a useful tool and this approach should also be followed to study the ion channels present in the basal membrane, which are even much less known. Application of the patch-clamp technique to the intact tissue was reported to be difficult in terms of gigaseal formation (Brown et al., 1993). In addition, syncytiotrophoblast tissue cannot be maintained in culture, and use of differentiating cytotrophoblast cells as an alternative source of ion channels seems inappropriate as these cells might not attain the same degree of differentiation as they do in the placental syncytium at term (Hoshina et al., 1985). Nevertheless, even though the reconstitution of native membrane fragments on planar lipid bilayers allowed the identification and characterization of a novel channel (this paper), it should be also borne in mind that vesicle isolation procedures might have caused the loss of cellular constituents (cytosolic factors, cytoskeletal proteins, ancillary subunits) that could be important for normal channel function (Rossier, 1998).

Physiological Role

Based on the presented results, we can only speculate about a physiological role for this channel. Clearly, the only peculiarity with some pharmacological interest is the channel's sensitivity to La^{3+}, which is highly characteristic (though, certainly, not indicative) of mechanosensitive channels (Yang & Sachs, 1989; Caldwell, Clemo & Baumgarten, 1998). Mechanosensitive channels have been described in a variety of epithelia where they were suggested to act as swelling-activated channels during cell-volume regulation. Most cell types, including the syncytiotrophoblast at term (Shennan, McNeillie & Curran, 1993), undergo an increase in volume when exposed to hyposmotic conditions. This initial swelling (caused by the influx of water) is followed by an efflux of intracellular osmolytes (K^+, Cl^-, amino acids, 6-carbon polyols) and osmotically obliged water which allows the cell to recover its initial size, a process known as regulatory volume decrease (RVD). During RVD, mechanosensitive nonselective cation channels are proposed to open upon cell swelling catalyzing the influx of Na^+ and Ca^{2+} which, in turn, activate K^+ and Cl^- efflux through Ca^{2+}-activated K^+ or Cl^- channels. Our reversal potentials measurements in experiments conducted in the presence of different chloride-based salts suggest that the placental cation-selective channel is also readily permeable to the other monovalent and divalent cations, in addition to K^+. Electrophysiological experiments have failed, however, to demonstrate the existence of Ca^{2+}-activated K^+ channels in the syncytiotrophoblast apical membrane but it is possible that these ion-selective pathways exist in the basal membrane. The Ca^{2+}-sensitivity of the apical Cl^- channels has not been studied thus far. This indirect involvement of stretch-activated channels in regulatory volume decrease, coupling the mechanical deformation of the cell to an increase in Ca^{2+}, has also been suggested in a variety of tissues such as choroid plexus (Christensen, 1987), renal proximal tubule cells (Hunter, 1990; Filipovic & Sackin, 1991, 1992), brain capillary endothelial cells (Popp et al., 1992), and GH_3 cells (Chen et al., 1996). Admittedly, though, we do not have any experimental evidence for the channel being mechanosensitive. However, as planar lipid bilayers are tension clamped (Sachs, 1997), attempts to modulate bilayer tension (for example by imposing a transmembrane hydrostatic pressure gradient) as a means of regulating the activity of the channel, would have been futile. Patch-clamp experiments will be needed to address this issue conclusively.

Some other roles for this nonselective cation channel such as participation in the transepithelial transfer of solutes between mother and fetus, and in the establishment of the rather depolarized microvillous membrane potential (median $\cong -22$ mV, Greenwood, Boyd & Sibley, 1993) cannot be ruled out. The extent to which this channel would contribute to these processes depends on its probability of being open in-vivo. To address this issue, we will need to know the factors that control channel opening (which may include situations other than cell-swelling), and the degree to which this channel gates spontaneously.

Within the framework of the RVD response, it is also possible that at least one of the two Cl^- channels described in the placental microvillous membrane (Grosman et al., 1997) acts as a pathway for Cl^- and negatively charged osmolyte efflux, as recently suggested (Birdsey et al., 1999). Several Cl^- channels have been shown to fulfill this role in other, epithelial and nonepithelial, tissues (Kirk, 1997).

Single-Channel Behavior

Kinetic heterogeneity has been reported for almost every ion channel characterized at the single-channel level. However, data selection procedures usually succeed in separating the current traces in more homogeneous data subsets that are more appropriate for functional studies. For the particular case of the placental cation-selective channel described in this paper, we could not find any straightforward criterion to classify the recordings as belonging to one class or another. Instead, we can only state that no simple kinetic model accounts for the channel's recorded behavior. By simulating single-channel recordings we arrived at the conclusion that we have to invoke the occurrence of temporal changes in the transition rates of a multistate linear kinetic scheme to account for many aspects of this channel's behavior in a parsimonious manner. This avoids the need of resorting to more complicated models where a different conformational change underlies each current transition. The hypothesized spontaneous changes in the transition rates between states, however, have eluded every attempt to be experimentally controlled, and represent the next intriguing issue in understanding how this novel channel gates.

The similarities between the single-channel properties of these nonselective cation channels and the maxi-Cl^- channels present in the placental microvillous membrane (other than the ion selectivity and sensitivity to blockers, of course) are remarkable (Grosman et al., 1997). Clearly, both have large conductances, multiple conductance states, complex kinetics, and unstable kinetics. However, the relationship between this particular channel behavior and the physiology of syncytial epithelia (if any) remains unknown.

As mentioned earlier, planar lipid bilayers are tension clamped. Due to the excess lipid available in the "torus" their tension does not change even when subjected to a transmembrane pressure gradient. Yet, the fact that the described channel was active in planar lipid bilayers is not in conflict with its proposed mechanosen-

sitivity. In eukaryotes, mechanical forces are suggested to reach the channel through the cortical cytoskeleton (Sachs, 1997; Sachs & Morris, 1998) which, very likely, underwent alterations during the membrane-vesicle isolation procedures. Thus, it is conceivable that some cytoskeletal disruption could have rendered the channel tonically active. Furthermore, planar lipid bilayers are under a substantial intrinsic tension which could be sufficient to activate the channel even "at rest" (Sachs, 1997). Finally, background activity could be expected as some stretch-activated channels (Sackin & Palmer, 1987; Chen et al., 1996) display some degree of spontaneous gating.

This work was partially supported by grants from the University of Buenos Aires and CONICET (Argentina) to I.L.R., and from the University of Buenos Aires to C.G. We thank Dr. Larry Palmer for critically reading the manuscript, and Mrs. Marisa Battelli de González Avila for technical assistance.

References

Alvarez, O., Benos, D., Latorre, R. 1985. The study of ion channels in planar lipid bilayer membranes. *J. Electrophysiol. Tech.* **12:**159–177

Birdsey, T.J., Boyd, R.D., Sibley, C.P., Greenwood, S.L. 1999. Effect of hyposmotic challenge on microvillous membrane potential in isolated human placental villi. *Am. J. Physiol.* **276:**R1479–1488

Booth, G.A., Olaniyan, R.O., Vanderpuye, O.A. 1980. An improved method for the preparation of human placental syncytiotrophoblast microvilli. *Placenta* **1:**327–336

Brown, P.D., Greenwood, S.L., Robinson, J., Boyd, R.D.H. 1993. Chloride channels of high conductance in the microvillous membrane of term human placenta. *Placenta* **14:**103–115

Byrne, S., Glazier, J.C., Greenwood, S.L., Mahendran, D., Sibley, C.P. 1993. Chloride transport by human placental microvillous membrane vesicles. *Biochim. Biophys. Acta* **1153:**122–126

Caldwell, R.A., Clemo, H.F., Baumgarten, C.M. 1998. Using gadolinium to identify stretch-activated channels: technical considerations. *Am. J. Physiol.* **275:**C619–C621

Chen, Y., Simasko, S.M., Niggel, J., Sigurdson, W.J., Sachs, F. 1996. Ca^{2+} uptake in GH_3 cells during hypotonic swelling: the sensory role of stretch-activated ion channels. *Am. J. Physiol.* **270:**C1790–C1798

Christensen, O. 1987. Mediation of cell volume regulation by Ca^{2+} influx through stretch-activated channels. *Nature* **330:**66–68

Faller, D.P., O'Reilly, C.M., Ryan, M.P. 1994. Amiloride-sensitive sodium uptake into human placental brush border membrane vesicles. *Biochem. Pharmacol.* **47:**757–761

Filipovic, D., Sackin, H. 1991. A calcium-permeable stretch-activated cation channel in renal proximal tubule. *Am. J. Physiol.* **260:**F119–F129

Filipovic, D., Sackin, H. 1992. Stretch- and volume-activated channels in isolated proximal tubule cells. *Am. J. Physiol.* **262:**F857–F870

Gaunt, M., Ockleford, C.D. 1986. Microinjection of human placenta. II: Biological application. *Placenta* **7:**325–331

Greenwood, S.L., Boyd, R.D.H., Sibley, C.P. 1993. Transtrophoblast and microvillus membrane potential difference in mature intermediate human placental villi. *Am. J. Physiol.* **265:**C460–C466

Grosman, C., Mariano, M.I., Bozzini, J.P., Reisin, I.L. 1997. Properties of two multisubstate Cl^- channels from human syncytiotrophoblast reconstituted on planar lipid bilayers. *J. Membrane Biol.* **157:**83–95

Grosman, C., Reisin, I.L. 1996. Nonselective cation channels from apical plasma membranes of human term placenta reconstituted on planar lipid bilayers. *Biophys. J.* **70:***A*199 (*Abstr.*)

Hoshina, M., Boothby, R., Hussa, R., Pattillo, R., Camel, H.M., Boime, I. 1985. Linkage of human chorionic gonadotrophin and placental lactogen biosynthesis to trophoblast differentiation and tumorigenesis. *Placenta* **13:**163–172

Hunter, M. 1990. Stretch-activated channels in the basolateral membrane of single proximal cells of frog kidney. *Pfluegers Arch.* **416:**448–453

Hunter, M., Giebisch, G. 1987. Multi-barrelled K channels in renal tubules. *Nature* **327:**522–524

Illsley, N.P., Sellers, M.C. 1992. Ion conductances in the microvillous and basal membrane vesicles isolated from human placental syncytiotrophoblast. *Placenta* **13:**25–34

Kirk, K. 1997. Swelling-activated organic osmolyte channels. *J. Membrane Biol.* **158:**1–16

Krouse, M.E., Schneider, G.T., Gage, P.W. 1986. A large anion-selective channel has seven conductance levels. *Nature* **319:**58–60

Popp, R., Hoyer, J., Meyer, J., Galla, H.-J., Gögelein, H. 1992. Stretch-activated nonselective cation channels in the antiluminal membrane of porcine cerebral capillaries. *J. Physiol.* **454:**435–449

Riquelme, G., Parra, M. 1999. Regulation of human placental chloride channel by arachidonic acid and other cis unsaturated fatty acids. *Am. J. Obstet. Gynecol.* **180:**469–475

Riquelme, G., Stutzin, A., Barros, L.F., Liberona, J.L. 1995. A chloride channel from human placenta reconstituted into giant liposomes. *Am. J. Obstet. Gynecol.* **173:**733–738

Rossier, B.C. 1998. Mechanosensitivity of the epithelial sodium channel (ENaC): controversy or pseudocontroversy? *J. Gen. Physiol.* **112:**95–96

Sachs, F. 1997. Mechanical transduction by ion channels: How forces reach the channel. *Society of General Physiologists Series.* **52:**209–218

Sachs, F., Morris, C.E. 1998. Mechanosensitive ion channels in nonspecialized cells. *In:* Reviews of Physiology, Biochemistry and Pharmacology. M.P. Blaustein, R. Greger, H. Grunicke, R. Jahn, L.M. Mendell, A. Miyajima, D. Pette, G. Schultz, and Schweiger, editors. pp. 1–78. Springer, Berlin

Sackin, H., Palmer, L.G. 1987. Basolateral potassium channels in renal proximal tubule. *Am. J. Physiol.* **253:**F476–F487

Shennan, D.B., Boyd, C.A.R. 1987. Ion transport by the placenta: a review of membrane transport systems. *Biochim. Biophys. Acta* **906:**437–457

Shennan, D.B., McNeillie, S.A., Curran, D.E. 1993. Stimulation of taurine efflux from human placental tissue by a hypoosmotic challenge. *Exp. Physiol.* **78:**843–846

Sibley, C.P., Birdsey, T.J., Brownbill, P., Clarson, L.H., Doughty, I., Glazier, J.D., Greenwood, S.L., Hughes, J., Jansson, T., Mylona, P., Nelson, D.M., Powell, T. 1998. Mechanisms of maternofetal exchange across the human placenta. *Biochem. Soc. Trans.* **26:**86–91

Stulč, J. 1989. Extracellular transport pathways in the haemochorial placenta. *Placenta* **10:**113–119

Stulč, J. 1997. Placental transfer of inorganic ions and water. *Physiol. Rev.* **77:**805–836

Yang, X.C., Sachs, F. 1989. Block of stretch-activated ion channels in *Xenopus* oocytes by gadolinium and calcium ions. *Science* **243:**1068–1071